

COVER PAGE

Document downloaded by @DAEL

Fri Nov 27 14:54:23 2026
For personal use

When automatic English translation is provided, only the original document is authentic.
The EAA cannot be held responsible of any translation error

Bibliographical reference

Plate Silencers for Broadband Low Frequency Sound Attenuation, Roman Kisler and Ennes Sarradj, Acta Acustica **vol. 104** (Number 3), 2018, pp. 521-527

DOI
https://doi.org/10.3813/AAA.919194

Acta Acustica united with Acustica
Vol. 104 (2018) 521 – 527

Technical and Applied Papers
DOI 10.3813/AAA.919194

Plate Silencers for Broadband Low Frequency Sound Attenuation

Roman Kisler[1], Ennes Sarradj[2]
[1] Chair of Technical Acoustics, Brandenburg University of Technology Cottbus-Senftenberg, Siemens-Halske-Ring 14, 03046 Cottbus, Germany. roman.kisler@tu-berlin.de
[2] Institute of Fluid Dynamics and Engineering Acoustics, Technische Universität Berlin, Einsteinufer 25, 10587 Berlin, Germany

Summary
An efficiency improvement for the implementation of a semi-analytical model of plate silencers in ducts is presented in this work. It is shown that a high approximation quality can be maintained even if the computation effort is reduced significantly. Thus, preliminary designs of plate silencers for specific purposes can be conducted with little effort. In addition, the accelerated implementation is utilized to perform an extensive parameter variation in order to find a best case configuration of silen properties and corresponding design rules. The results of these studies show that a tuning of plate and geometry parameters allow for substantial increases in a silencer's attenuation performance.

PACS no. 43.20.Hq, 43.40.Tm, 43.50.Gf

1. Introduction

Plate silencers are expansion chambers fully covered with a plate. They have many advantages to silencers made of porous material or perforated surfaces. They can be exposed to contaminated air, heat, frost and humidity without being damaged. Due to their smooth surfaces, their flow resistance is comparatively low.

There are basically three common methods available to model the physical behavior of plate silencers. Mechel [1] proposed a method to determine the absorption coefficient of resonating plates with perpendicular sound incidence. Combined with the empirical Piening formula it matches the absorption coefficient linearly with the transmission loss [2], which is a very rough estimate due to the model's empirical basis [3]. Another approach is the numerical investigation (e.g. with the finite element method (FEM)), which has the drawback of not giving insight into the underlying physical principle of the plate silencer and requires big computational effort. It does, however, enable the investigation of much more complex systems than empirical or, as following, analytical solutions do. The third method is a semi-analytical model which solves the bending differential equation by a discretization of the modal domain of both the plate and the enclosed cavity.

This more sophisticated semi-analytical model was introduced by Huang [4] with a modal analysis of a drumlike silencer. He continued his work on this type of silencers with parameter studies [5] and an extension to three dimensions [6, 7]. In [8, 9, 10], Wang examined the same model in order to further optimize the silencer's properties such as the distribution of the plate's spatial bending stiffness to improve its performance.

Yet, the results were obtained by the comparison of a limited amount of parameter variations due to the high computational effort of the implementation. The present work aims at a more efficient formulation of the model to enable faster calculation and extensive parameter studies over a broad frequency range.

First, the underlying physical model is described. Secondly, the adjustable approximation quality is analyzed to show that a lower discretization of the modal domain is sufficient in order to achieve little error. Finally, the implementation is used to conduct an extensive parameter variation to find design rules which allow for low frequency, broadband transmission losses.

2. Physical model

Following [9], Figure 1 depicts the generic physical principle of a plate silencer. The sound waves propagate from left to right and thereby graze the plates which are wall-mounted onto two opposite walls of the duct and are clamped on both sides. Behind each plate there is a closed cavity filled with air. The sound pressure excites the plate to vibrate due to the pressure difference between upper and lower side of the plate. These vibrations are highly coupled with the sound field inside the enclosed cavity, which itself is induced by the plate's vibration. Ultimately, the plate's vibration radiates a portion of the incoming sound

Received 13 June 2017,
accepted 24 February 2018.

© S. Hirzel Verlag · EAA

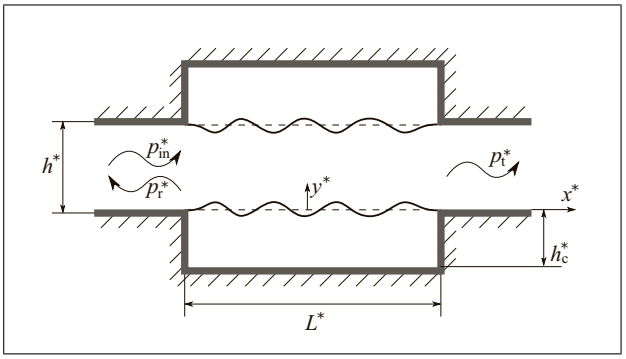

Figure 1. Model of a two-sided plate resonator as a silencer, see [9].

energy, depending on the resonant frequencies of the coupled plate-air system, back to the inlet and thus result in transmission loss.

In the following, the current semi-analytical model from [9] will be briefly described. First, all required physical properties of the setup are made dimensionless in order to keep the calculated results scalable between different applications:

$$h_p = \frac{h_p^*}{h^*} \qquad B = \frac{B^*}{\rho_0^*(c_0^*)^2(h^*)^3} \qquad h_{\mathrm{c}} = \frac{h_{\mathrm{c}}^*}{h^*}$$
$$L = \frac{L^*}{h^*} \qquad V = \frac{V^*}{c_0^*} \qquad m'' = \frac{m''^*}{\rho_0^* h^*}$$
$$p = \frac{p^*}{\rho_0^*(c_0^*)^2} \qquad f = f^*\frac{h^*}{c_0^*},$$

where h_p^* the plate thickness, B^* the bending stiffness, h_{c}^* the cavity height, L^* the cavity length, V^* the normal plate velocity, m''^* the plate's areal density, p^* the sound pressure, and f^* the frequency. Dimensioned parameters are marked by an asterisk. The reference values are chosen as the channel height h^*, the density ρ_0^* of air and the speed of sound c_0^*. For the model only plane waves are assumed. Hence, the highest allowed frequency is limited to the cut-off condition of the channel which is $f_c = 0.5$.

To find a solution for this underlying physical problem, the differential equation for bending waves of an Euler beam is solved. This model is restricted to the two-dimensional case, as Huang found only small differences in comparing the three-dimensional case with the former [6]. Therefore, the two-dimensional model is sufficient for preliminary estimates and designs of the desired transmission loss.

The bending differential equation is transformed into a system of linear equations by applying the standard Galerkin method, in which the plate velocity is substituted with a series expansion using particular orthogonal base functions.

$$\left(\underline{\mathbf{L}} + \underline{\mathbf{Z_c}} + \underline{\mathbf{Z}_+}\right) \cdot \mathbf{V} = -\mathbf{I}. \tag{1}$$

The variable $\underline{\mathbf{L}}$ is a diagonal matrix comprising material parameters. The intrinsic material damping is neglected in this study, but it can be implemented easily using the Raleigh damping model [7]. $\underline{\mathbf{Z_c}}$ corresponds to the quadratic matrix of the modal impedances on the cavity side and $\underline{\mathbf{Z}_+}$ to the modal impedances on the duct side. They strongly depend on the assumed boundary conditions. Each entry of these matrices is approximated by a summation over R and S orthogonal cavity and duct modes,

$$Z_{cjl} = \sum_r^R \sum_s^S Z_{cjl,rs}, \quad Z_{+jl} = \sum_r^R Z_{+jl,r}. \tag{2}$$

On the right hand side of Equation (1), $\mathbf{I}$ describes the modal amplitudes of the incoming sound waves. The vector $\mathbf{V}$ stands for the amplitudes of the plate velocity modes. A base function vector $\boldsymbol{\varphi}(x)$ is chosen from the in-vacuo eigenmodes of an Euler beam with clamped edges.

Thus, the normal plate velocity can be approximated as

$$V_N(x) = \mathbf{V} \cdot \boldsymbol{\varphi}(x). \tag{3}$$

N is the number of plate modes that shall be taken into account and $\mathbf{V} \in \mathbb{C}^N$ is the vector of amplitudes of the plate's in-vacuo eigenmodes. If N would tend to infinity, $N \to \infty$, the plate velocity would be reconstructed without error. For realistic calculation the considered number of eigenmodes needs to be limited which, together with R and S, defines the approximation quality of this entire model. In addition, N strongly determines the required computation time of an implementation, as it sets the size of the main system of linear Equations (1).

With the solution of this system of linear equations the upstream and downstream radiated sound from the plate can be calculated, as demonstrated in [8]. This allows for the determination of reflected and transmitted sound powers P_r, P_t. Due to the neglected damping within this model, there is no absorbed sound power, i.e. $P_a = 0$. That enables the calculation of the required transmission loss TL for each frequency.

$$TL = 10\log_{10}\left(\frac{P_{\mathrm{in}}}{P_{\mathrm{t}}}\right)\mathrm{dB} = 20\log_{10}\left(\frac{p_{\mathrm{in}}}{p_{\mathrm{t}}}\right)\mathrm{dB}. \tag{4}$$

The variables p_{in} and p_{t} are the complex amplitudes of the sound pressure from the incoming sound source at the inlet and from the transmitted sound at the outlet, respectively. They are visualized in Figure 1. With the amplitudes $\mathbf{V}$ from the linear system of equations in (1), TL can be calculated as

$$TL(f) = -20\log_{10}\left|1 + \mathbf{V}(f) \cdot \mathbf{T}(f)\right|, \tag{5}$$

where $\mathbf{T}$ corresponds to modal weights of the plate's sound radiation.

3. Approximation quality

This section aims at determining the most reliable trade-off between computation speed and approximation quality. Analysis in [5] showed that a minimum number of plate

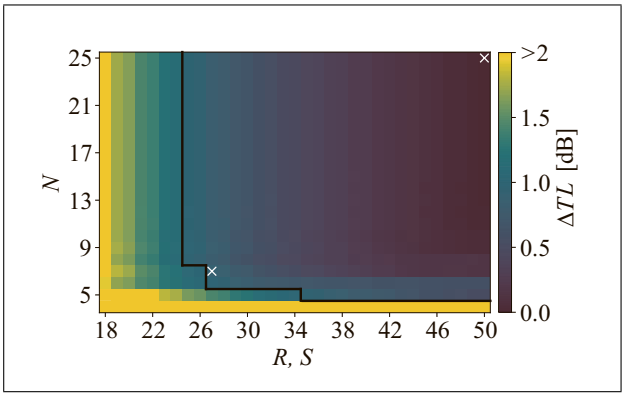

Figure 2. Maximum absolute deviation ΔTL from the resolution $(N, R, S) = (25, 50, 50)$ proposed in [9]. The white crosses mark the maximum $(25, 50, 50)$ and sufficient $(7, 27, 27)$ modal resolution. The black line indicates the border of $\Delta TL = 1$ dB.

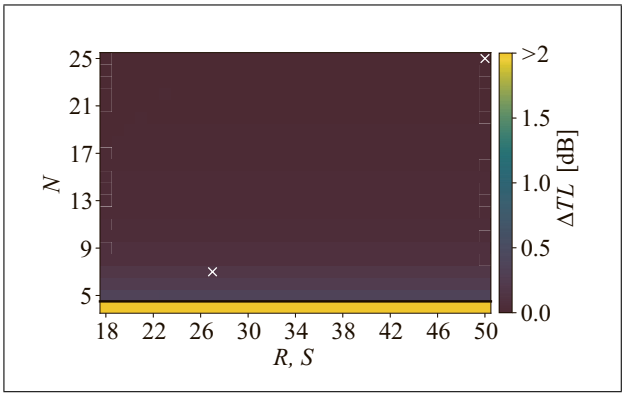

Figure 3. Maximum absolute deviation ΔTL for the lower parameter bounds $(h_c, m'', B) = (0.15, 0.08, 10^{-9})$. The white crosses mark the maximum $(25, 50, 50)$ and sufficient $(7, 27, 27)$ modal resolution. The black line indicates the border of $\Delta TL = 1$ dB.

modes of $N = 25$ and $R = S = 50$ cavity modes are necessary to ensure a sufficient approximation quality.

This type of analyses is repeated here with an own validated implementation of the model from [8]. As a first validation reference the test case from [10] was used. Its parameters are as follows: $L = 5, h_c = 1, m'' = 2.4, B = 0.11, f \in [0,\ 0.25]$, and two opposite plates with coupled cavities and no flow considered. The algorithm was run for each permutation of the mode number tuple $(N,\ R,\ S)$, with $S = R$ for simplicity. The maximum absolute deviation ΔTL in the TL frequency response between each run and the reference was determined.

Figure 2 illustrates the results. They show that far less mode numbers than $(N, R, S) = (25, 50, 50)$ are required for high precision over the entire analyzed frequency spectrum of $f \in [0,\ 0.25]$. As the main aim of the plate silencer is to achieve broadband low frequency sound attenuation, frequencies beyond $f > 0.25$ are disregarded. The black line depicts the border between a maximum error bigger than 1 dB on the left hand side and less than 1 dB on the right hand side. Even a mode pair of $(N, R, S) = (5, 35, 35)$ is sufficient to achieve an error less than 1 dB. However, the Figure also shows that a resolution of just five plate modes never reaches the maximum reference precision, no matter how many cavity modes are taken into account. As the calculation time mainly depends on the number of considered plate modes rather than the number of cavity modes, the pair with the smallest amount of plate modes is most efficient for this specific case. As seven plate modes are capable of almost achieving the highest accuracy with $R = 50$, the mode pair $(N, R, S) = (7, 27, 27)$ is chosen for future analysis as the best trade-off between accuracy and computational effort. A further increase of the considered plate mode numbers does not improve the approximation quality significantly. Similar approximation results were achieved for other configurations of the material parameters as well.

Additionally, the results in Figure 2 imply that only the first seven plate modes are sufficiently excited and responsible for the relevant upstream sound radiation in this specific case.

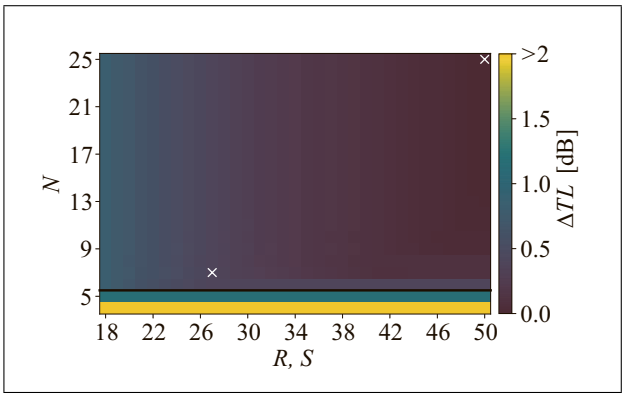

Figure 4. Maximum absolute deviation ΔTL for the upper parameter bounds $(h_c, m'', B) = (5, 17, 0.135)$. The white crosses mark the highest $(25, 50, 50)$ and sufficient $(7, 27, 27)$ modal resolution. The black line indicates the border of $\Delta TL = 1$ dB.

The previous analysis only covered a single set of system parameters. Hence, it has to be made sure that the reduction of the model size and its resulting error also holds for the remaining parameters considered in future analyses. Therefore, the maximum absolute deviation ΔTL is determined for two more cases. They represent the outer bounds of the parameter space which forms the basis for the parameter study in the next section, i.e. $(h_c, m'', B) \in \{(0.15, 0.08, 10^{-9}), (5, 17, 0.135)\}$. For both cases the same procedure for the determination of ΔTL is followed as before, yielding the results depicted in Figures 3 and 4. These two extreme cases allow for a smaller mode resolution than the parameter set used in Figure 2 to ensure an error less than 1 dB over the analyzed frequency range of $f \leq 0.25$. Additional error calculations for the optimal parameter sets that resulted from the parameter study in the upcoming section supported the outcome that $(N, R, S) = (7, 27, 27)$ mode orders are sufficient enough to achieve a high precision with a deviation of $\Delta TL \lessapprox 1$ dB.

The computational effort using a single commercial up-to-date CPU core was reduced by 95 % when using $(N, R, S) = (7, 27, 27)$ instead of $(N, R, S) = (25, 50, 50)$ given in [5]. With the simple Python implementation used here, the computation time for a single frequency took 1.88 seconds with $(25, 50, 50)$ modes and 0.094 seconds with $(7, 27, 27)$, on average.

In addition, a 2D FEM simulation was conducted with Actran, a commercial FEM software. A simulation for a single frequency required 0.19 seconds. Although the speed-up of the semi-analytical model compared to the FEM simulation still reaches a factor of 2, the Python implementation of the semi-analytical model is not computationally optimized for speed yet in contrast to the commercial FEM Software. If the implementation would be improved, an additional speed-up of at least 25 would be realistic, so that in consequence it would be 50 times faster that FEM. In conclusion, this overall speed-up makes extensive parameter studies more feasible, especially when additional computational parallelization is applied.

4. Parameter study

This parameter study aims at finding acoustically favorable material and geometry parameters. To characterize these properties of a chosen configuration a stop band SB is defined as a functional,

$$SB = \max \frac{f_\mathrm{u}}{f_\mathrm{l}}, \text{ with } TL\big(f \in [f_\mathrm{l},\ f_\mathrm{u}]\big) \geq TL_\mathrm{c}, \quad (6)$$

with f_u and f_l as the upper and lower frequency of the stop band, respectively. It determines the highest achievable bandwidth within the analyzed frequency spectrum where the transmission loss is above a specified threshold $TL > TL_\mathrm{c}$. This allows the comparison of the bandwidth performance between various silencer configurations. It also ensures that the resulting silencers achieve transmission losses within the stop band that are higher than with a chosen reference silencer, for example an expansion chamber of twice the size of the plate silencer (see the later definition of TL_c in (10)).

Figure 5 illustrates the definition of the stop band variable. It shows the transmission loss of the plate silencer, which has been utilized for determining the approximation quality of the model in section 3.

In the parameter study the most relevant parameters are varied: cavity height, plate's areal density and bending stiffness. The following variation intervals are analyzed,

$$h_\mathrm{c} \in [0.15,\ 5] \text{ with 44 samples}, \quad (7)$$
$$m'' \in [0.08,\ 17] \text{ with 32 samples}, \quad (8)$$
$$B \in [10^{-9},\ 0.135] \text{ with 64 samples}, \quad (9)$$

which gives altogether 90112 cases. These parameters were chosen with respect to realistic material and geometry values. A mean plug flow is disregarded here, though it is easily possible with this model [8]. Following [5], the length of the silencer is set to $L = 5$.

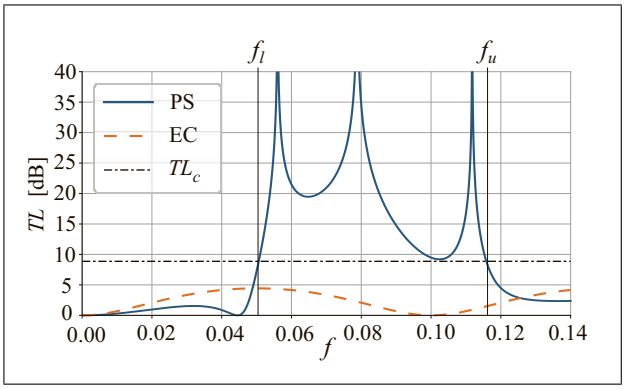

Figure 5. Visualization of the definition of the stop band SB. PS corresponds to the plate silencer, while EC corresponds to the transmission loss of an expansion chamber of equal size. In this example, TL_c is chosen to twice the value of $\max(TL_\mathrm{E})$ (see Equation 10), yielding $SB = 2.3$.

For the parameter study the criterion value TL_c needs to be specified. According to [4] and to this specific case the threshold is set to twice the maximum transmission loss of a basic expansion chamber TL_E, which is derived in detail in [11], with the same identical cavity height h_c. The threshold is defined as

$$TL_\mathrm{c} = 2 \cdot \max(TL_\mathrm{E}) \quad (10)$$
$$\max(TL_\mathrm{E}) = 10 \log_{10} \left(1 + \frac{1}{4}\left(\Lambda^{-1} - \Lambda\right)^2\right) \mathrm{dB} \quad (11)$$
$$\Lambda = 1 + 2h_\mathrm{c}, \quad (12)$$

where Λ is the ratio between the cross section of the chamber and the duct's cross section. Thus, Equation (11) shows that bigger cavity heights h_c yield a greater transmission loss maximum $\max(TL_\mathrm{E})$. That is why the corresponding adjustment of the criterion to the cavity height has high significance for the comparison of the resulting stop bands.

As the goal is to achieve high attenuation at lower frequencies, the analyzed bandwidth is limited to $f \in]0,\ 0.25]$ with 150 linearly distributed samples. This frequency range was chosen in order to restrict the analysis to low frequencies, below half the cut-off frequency of $f = 0.5$, so that the best possible transmission loss within this interval can be determined.

Figure 6 shows the dependency of the stop band from the plate's areal density and the cavity height at the six highest analyzed bending stiffnesses between $B = 0.031$ and $B = 0.135$.

As expected from [7], the widest stop band is achieved with a high bending stiffness. The image series shows that lower bending stiffnesses barely reach any sound attenuation better than that of a comparable expansion chamber. All lower bending stiffnesses analyzed within the chosen parameter space are less effective than the $B = 0.031$ case depicted in Figure 6. The results seen in this series lead to the conclusion, that plate silencers with high bending stiffnesses achieve better benefits at shallow cavity heights. On the other hand, the areal densities with the maximum

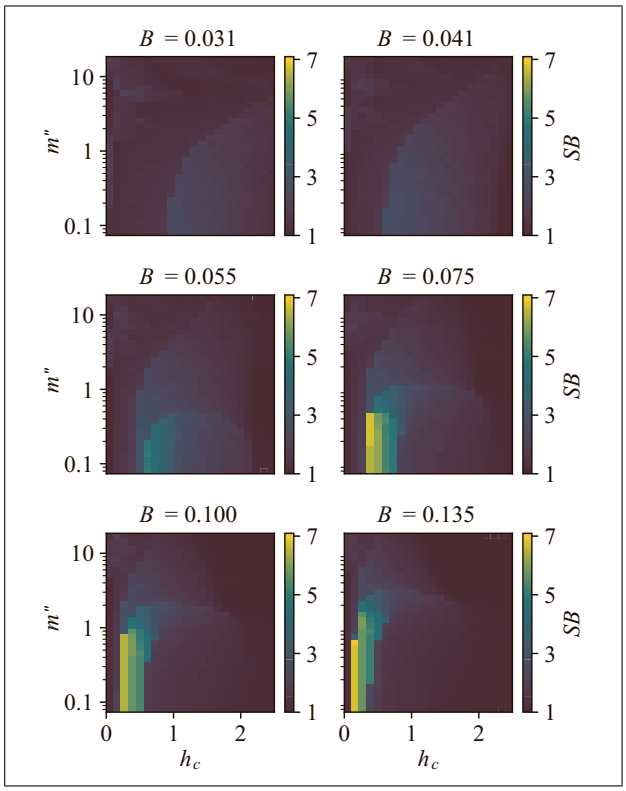

Figure 6. Result example: Stop band SB as a function of the areal density m'' of the plate and the cavity height h_c at a bending stiffness of $B = 0.075$.

stop bands do not exceed $m'' = 1$ for all considered bending stiffnesses. The maximum stop band of the parameter study with $SB \approx 7.1$ is reached with a cavity height of $h_c \approx 0.154$, a bending stiffness of $B \approx 0.135$ and an areal density of $m'' \approx 0.64$, as Figure 6 shows. Figure 7 depicts the transmission loss of the best case in comparison to an equally sized expansion chamber. It can be seen that the transmission loss between $f_l = 0.0345$ and $f_u = 0.25$ is at least twice as high as the maximum attenuation of an equally sized expansion chamber.

However, Figure 7 also reveals that the attenuation of the plate silencer is outperformed by the reference expansion chamber for frequencies lower than $f < 0.0345$. This corresponds to $f^* < 50$ Hz for duct heights higher than $h^* > 23.5$ cm and an induct temperature of 288 K. Thus, these cases only apply to very low frequency sound sources and very small ducts.

As a general conclusion, if enough building space is available for an use case ($h_c \geq 0.5$), lower bending stiffnesses $B < 0.075$ are recommended with lower stop bands as a trade off, but if the space is strongly limited ($h_c \leq 0.5$), plate resonators achieve their highest potential in terms of the stop band with highest possible bending stiffnesses, but with a lower overall transmission loss as a consequence.

Although Figure 6 indicates that configurations with $B < 0.075$ do not achieve sufficient attenuation, Figure 8 shows that the stop band still reaches a reasonable value of $SB \approx 3$. In addition, plate silencers with low bending stiffnesses allow for much wider variations of the cavity height

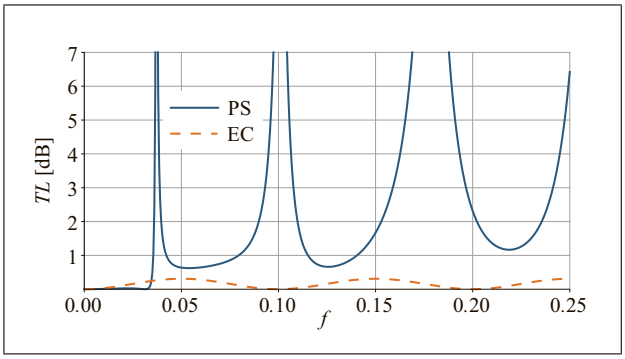

Figure 7. Transmission loss of the most beneficial case determined by the conducted parameter study. PS depicts the plate silencer, while EC shows the attenuation of the corresponding expansion chamber.

Table I. List of parameters for three plate silencer configurations.

	h_c	m''	B
I	1.000	1.000	0.070
II	0.500	0.080	0.075
III	0.154	0.637	0.135

and areal density without losing much performance, thus having higher tolerance.

Still, it has to be noted that lower cavity heights yield lower maximum values of possible transmission losses according to Equation (10). Figure 8 illustrates the difference between the calculated most beneficial case from Figure 6 and a less optimal case. The latter has been chosen in regard to achieving the widest stop band with a minimum transmission loss (TL_c) of 4 dB, yielding the following parameters: $B \approx 0.075$, $m'' = 0.08$ and $h_c = 0.5$. Figure 8 illustrates the trade off between wide stop band SB and high transmission loss. It compares three cases, one of which (I) is the optimal case determined in [9] with $SB = 2.8$ and a minimum transmission loss of $TL_c = 10$ dB within the stop band. The second configuration (II) is the most effective case for a threshold of $TL_c = 4$ dB with $SB = 6.2$. The third plate silencer (III) is the one with the highest determined stop band of $SB = 7.1$ in the parameter study. Table I lists their individual parameters. This comparison makes clear that high stop bands, as they are defined here, do not account for the minimum transmission loss that is possible with the corresponding cavity height. Although the best case of the parameter study (III) does give the highest benefit in comparison to its reference expansion chamber of twice the size, it is not able to achieve the absolute transmission loss of bigger plate silencers.

To further understand the influence of the cavity height on the performance of the plate silencer, the maximum possible stop band is considered in relation to the transmission loss threshold TL_c, which is only depending on the cavity height of an equally sized expansion chamber (see Equation 10). This relation is displayed in Figure 9. It shows that the maximum possible stop band decreases significantly from $TL_c \approx 2.5$ dB on. In detail this implies that

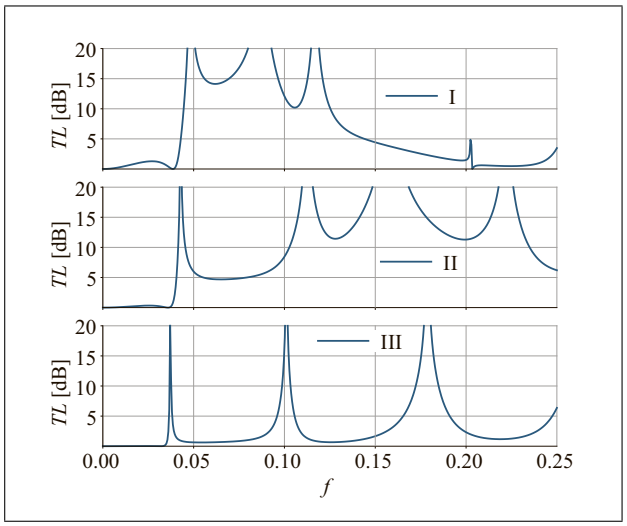

Figure 8. Comparison of the transmission loss of three plate silencers with different parameters taken from Table I.

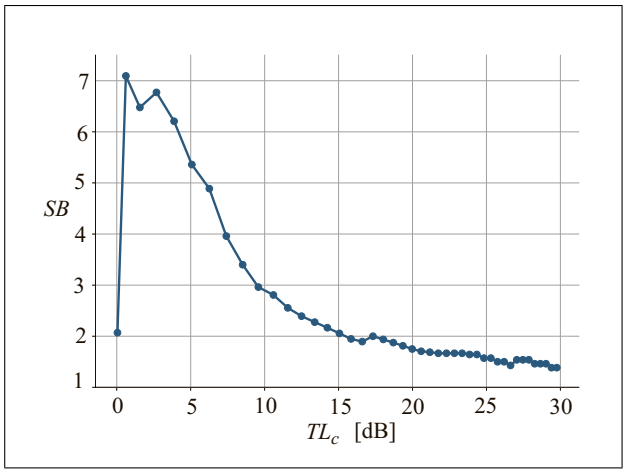

Figure 9. Dependency of the maximum possible stop band SB on the transmission loss criterion TL_c of the corresponding expansion chamber.

higher transmission losses and accordingly bigger cavity heights attain narrower stop bands. If, for example, at least two octaves ($SB \geq 4$) are desired to be attenuated by a plate silencer, the cavity height is required to be higher than $h_c \geq 0.86$, so that the transmission loss of such a silencer will not fall below 7.5 dB within the stop band.

While the results in [9] show that for $h_c = 1$ the widest stop band is $SB = 2.81$ (which is confirmed in Figure 9), Figure 6 indicates that a much wider stop band is possible for cavity heights of $h_c < 1$ and for a wider range of areal densities.

A further analysis of higher frequencies up until $f = 0.5$ for two exemplary plate configurations II and III (see Table I) shows an extensively broader stop band of up to $SB = 13.9$ in Figure 10, which corresponds to almost four octaves. Even the most efficient configuration (silencer II from Table I) with a cavity height of $h_c = 0.5$ is capable of attenuating a stop band of $SB = 12.4$ when the entire plane wave frequency range is considered. In conclusion,

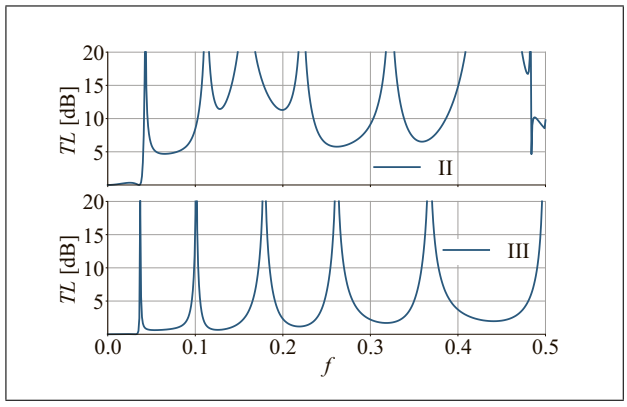

Figure 10. Sound attenuation of two exemplary plate silencers II and III (see Table I) for frequencies up to the first cut-off frequency $f_c = 0.5$.

although the performance analysis of all parameter tuples only applied to frequencies until $f = 0.25$, certain plate silencer configurations show high and broadband attenuation up until the cut-off frequency.

5. Conclusion

This study was able to demonstrate that a sufficiently precise modeling of plate silencers is possible by regarding only the first seven plate in-vacuo eigenmodes and 27×27 cavity modes. Thereby, the computation time of the existing semi-analytical model is significantly reduced by 95 % compared to the full resolution used in literature, i.e. $(25,\ 50,\ 50)$. This advantage made it possible to conduct an extensive parameter study with over 90112 cases in order to identify favorable parameters for high transmission losses.

Therefore, an expansion chamber twice the size of the examined plate silencer was utilized as the reference silencer. The results of this conducted parameter study show that, even though a high bending stiffness is required, the areal density does not need to be minimized in order to gain higher and more broadband transmission losses. In fact, it reaches its peak performance with a stop band of $SB = 7.1$. An analysis of the efficiency of plate silencers revealed that it decreases with higher cavity heights. Thus, such plate silencers still do achieve higher transmission losses, but at the expense of the widest possible stop band.

In addition, it was possible to show that the best trade-off between a broadband, low frequency sound attenuation and high transmission losses can be achieved with a cavity height of $h_c = 0.5$ which yields a stop band of $SB = 6.2$ and a minimum transmission loss of 4 dB and above for higher frequencies. The results also lead to the general conclusion that certain combinations of parameters can yield a significant and broadband transmission loss in the low frequency range for $f \in [0.04,\ 0.25]$. Certain configurations of plate silencers achieve even wider stop bands when frequencies up to $f = 0.5$ are taken into account. Besides, the results of the parameter study also lead to a

recommended value for the maximum effective areal density, i.e. $m'' = 1$, at arbitrary bending stiffnesses. In conclusion, these results demonstrate that substantial improvements over the expansion chamber are easily possible by only installing a well designed plate between cavity and duct.

Acknowledgment

The work presented here was funded by the German Federal Ministry for Economic Affairs and Energy due to a resolution of the Parliament of the Federal Republic of Germany.

References

[1] F. Mechel, N. Kiesewetter: Schallabsorber aus Kunststoff-Folie. Acta Acustica united with Acustica **47** (1981) 83–88.

[2] W. Piening: Schalldämpfung der Ansauge- und Auspuffgeräusche von Dieselanlagen auf Schiffen. VDI-Zeitschrift **81** (1937) 770–776.

[3] H. V. Fuchs: Applied Acoustics: Concepts, Absorbers, and Silencers for Acoustical Comfort and Noise Control: Alternative Solutions-Innovative Tools-Practical Examples. Springer Science & Business Media, 2013.

[4] L. Huang: Modal analysis of a drumlike silencer. The Journal of the Acoustical Society of America **112** (2002) 2014–2025.

[5] L. Huang: Parametric study of a drum-like silencer. Journal of Sound and Vibration **269** Elsevier (2004) 467–488.

[6] L. Huang, Y. Choy: Vibroacoustics of three-dimensional drum silencer. The Journal of the Acoustical Society of America **118** (2005) 2313–2320.

[7] L. Huang: Broadband sound reflection by plates covering side-branch cavities in a duct. The Journal of the Acoustical Society of America **119** (2006) 2628–2638.

[8] C. Wang: Development of a broadband silencer in flow duct. PhD thesis. The Hong Kong Polytechnic University, 2008.

[9] C. Wang, J. Han, L. Huang: Optimization of a clamped plate silencer. The Journal of the Acoustical Society of America **121** (2007) 949–960.

[10] C. Wang, L. Cheng, L. Huang: Realization of a broadband low-frequency plate silencer using sandwich plates. Journal of Sound and Vibration **318** (2008) 792–808.

[11] M. Möser: Engineering Acoustics. Springer, Berlin, Germany, 2009.